



An integrated numerical method for wind turbine flow simulation, sound generation and propagation

Zhu, Wei Jun; Cao, Jiufa; Barlas, Emre; Shen, Wen Zhong; Zhang, Lei; Sun, Zhenye; Yang, Hua; Xu, Haoran

Published in:

Journal of Physics: Conference Series (Online)

Link to article, DOI:

[10.1088/1742-6596/1037/2/022002](https://doi.org/10.1088/1742-6596/1037/2/022002)

Publication date:

2018

Document Version

Publisher's PDF, also known as Version of record

[Link back to DTU Orbit](#)

Citation (APA):

Zhu, W. J., Cao, J., Barlas, E., Shen, W. Z., Zhang, L., Sun, Z., ... Xu, H. (2018). An integrated numerical method for wind turbine flow simulation, sound generation and propagation. *Journal of Physics: Conference Series (Online)*, 1037(2), [022002]. DOI: 10.1088/1742-6596/1037/2/022002

General rights

Copyright and moral rights for the publications made accessible in the public portal are retained by the authors and/or other copyright owners and it is a condition of accessing publications that users recognise and abide by the legal requirements associated with these rights.

- Users may download and print one copy of any publication from the public portal for the purpose of private study or research.
- You may not further distribute the material or use it for any profit-making activity or commercial gain
- You may freely distribute the URL identifying the publication in the public portal

If you believe that this document breaches copyright please contact us providing details, and we will remove access to the work immediately and investigate your claim.

PAPER • OPEN ACCESS

An integrated numerical method for wind turbine flow simulation, sound generation and propagation

To cite this article: Wei Jun Zhu *et al* 2018 *J. Phys.: Conf. Ser.* **1037** 022002

View the [article online](#) for updates and enhancements.

Related content

- [Integrated design optimization of wind turbines with noise emission constraints](#)
P Bortolotti, CR Sucameli, A Croce *et al.*
- [CFD analysis for siting of wind turbines on high-rise buildings](#)
K Veena, V Asha, C Arshad Shameem *et al.*
- [Methodological approach to simulation and choice of ecologically efficient and energetically economic wind turbines \(WT\)](#)
Vadim Bespalov, Natalya Udina and Natalya Samarskaya



IOP | ebooks™

Bringing you innovative digital publishing with leading voices to create your essential collection of books in STEM research.

Start exploring the collection - download the first chapter of every title for free.

An integrated numerical method for wind turbine flow simulation, sound generation and propagation

Wei Jun Zhu^{1,2}, Jiufa Cao^{1,*}, Emre Barlas², Wen Zhong Shen², Lei Zhang³, Zhenye Sun¹, Hua Yang¹, Haoran Xu¹

¹ School of hydraulic energy and power engineering, Yangzhou University, China

² Technical University of Denmark, Lyngby 2800, Denmark

³ Institute of Engineering Thermophysics, Chinese Academy of Sciences, Beijing 100190, China

Email: jfcao@yzu.edu.cn

Abstract. The scope of the paper is to present an efficient numerical method that predicts: (a) wind turbine aerodynamic loads and power; (b) wind turbine noise source; (c) long distance wind turbine noise source propagation. The numerical methods involved in this study are a combination of Computational Fluid Dynamics (CFD) and wind turbine aeroacoustic methods. The results from the CFD simulation provide necessary information of wind turbine power and thrust etc. The 2D Actuator Disc (AD) theory is applied for such a purpose. The computational efficiency becomes very high while using a steady 2D CFD approach. The flow geometry at each blade element is required for wind turbine noise source calculations. The predicted wind turbine noise source is the starting field for long distance noise propagation model which is based on solving the Parabolic Equations (PE) in the frequency domain. Results showed that the integrated wind turbine flow-acoustic prediction method is capable of calculating wind turbine aerodynamic, aerodynamic noise source and long range sound propagation.

1. Introduction

Numerous methods exist for evaluation of wind turbine aerodynamics. The Blade Element Momentum (BEM) method [1] is the main engineering tool that predicts the aerodynamic loading for a single wind turbine. Ideally, the model accuracy increases with increasing model complexity and the simulation cost. The vortex wake (VW) methods and the CFD methods are more advanced tools that can predict both aerodynamic loads and the flowfield around wind turbines. The methods become more time consuming when the wake flow behind the wind turbines is longer. In the field of wind turbine aerodynamic study, the sophisticated methods called AD/AL/AS (Actuator Disc/Actuator Line/Actuator Surface) techniques are good trade-off between numerical accuracy and computational efficiency. Due to the high efficiency, the AD method [2] is applied in the current study. The rotor disc is assumed permeable and the external forces acting on the disc are added to the momentum equations of the Navier-Stokes (NS) equations. Considering Horizontal Axis Wind Turbines (HAWTs), there is an inherent axisymmetric characteristic of the rotor. In an ideal case, the 3D AD method can be reduced to a 2D formulation. If an axisymmetric boundary condition is applied to the NS equations, the resulted flowfield should be identical to the 3D flowfield. It is worth mentioning that the statement of axisymmetric only holds true for a turbine in uniform inflow condition without yawing, tilting effects etc.

The method behind the noise source simulation is the so-called BPM method [3,4]. As a novel technique used in the current work, the wind turbine noise source model is combined with a flow solver. The relative velocity and angle of attack obtained from the CFD simulation are the key input to



the wind turbine noise generation model. In the next step, wind turbine noise is predicted over long distance from the noise source position to receiver. The PE method [5,6] is applied with a wind turbine noise source as a major input. The noise propagation medium, which is an important factor that influences the propagation path, is given by the resulted CFD flowfield. Noise propagation in complex flowfield is known as an important issue of single wind turbines or wind farms. The influence of noise propagation under different atmospheric conditions were observed by Lee [7] and Heimann [8], where the PE method and ray-tracing method were applied by LEE and Heimann, respectively. Both studies show large noise variations with wind profile and atmospheric stability. Later on, PE method is applied in the numerical study of Barlas et al. [9], it was found that wind turbine noise propagation has various refraction patterns due to the existence of wind turbine wake flow. The intention of the current work is to integrate wind turbine flow field computation, noise source and propagation altogether. The mechanisms of noise propagation through multi-wind turbine wake is investigated.

The paper structure is as following: section 2 briefly describes the numerical methodology behind the flow, noise generation and noise propagation modelling; section 3 presents results from integrated flow-noise model; section 4 gives conclusions and some future works.

2. Methodology

The numerical techniques that involved in this study are described as follows: (1) RANS/AD wind turbine flow simulation; (2) BPM wind turbine noise source generation; (3) PE sound propagation.

2.1 RANS/AD method

The general equations of flow around a wind turbine are the incompressible NS equations with an external force term appears as momentum source:

$$\frac{\partial u_i}{\partial x_i} = 0 \quad (i = 1, 2) \quad (1)$$

$$\frac{\partial u_i}{\partial t} + u_j \frac{\partial u_i}{\partial x_j} = -\frac{1}{\rho} \frac{\partial P}{\partial x_i} + \frac{\partial}{\partial x_j} (\nu \frac{\partial u_i}{\partial x_j} - \overline{u_i u_j'}) + f_{ext} \quad (2)$$

$$-\rho \overline{u_i u_j'} = \mu_t \left(\frac{\partial u_i}{\partial x_j} + \frac{\partial u_j}{\partial x_i} \right) - \frac{2}{3} \rho k \delta_{ij} \quad (3)$$

where x_i and u_i are the displacement and velocity components in the inertial coordinate system. t is time, ρ is the density of fluid, P is the static pressure, ν is the molecular momentum viscosity coefficient, f_{ext} is the momentum source terms representing the aerodynamic forces on the rotor disc. In this study, the 3D-NS equation is reduced to 2D RANS/AD equations such that the computational efficiency is largely increased. Such an assumption is based on the axisymmetric property of the HAWTs.

As the disc is assumed permeable, the mass equation remains unchanged. In equation (2), an external force f_{AD} is added that represents aerodynamic loadings of wind turbine blades. To avoid numerical singularity, each volume force needs to be smoothly re-distributed. The practical way of smearing the force is to use the 1D Gaussian function such that the actual forces in the disc is redistributed along one direction. In the current model, each force element is smeared in the normal direction with a distance d away from the disc using the convolution and the smear force f' is computed as

$$f' = f_{AD} \otimes \eta^{1D} \quad (4)$$

$$\eta^{1D}(d) = 1 / (\epsilon \sqrt{\pi}) \exp[-(d / \epsilon)^2] \quad (5)$$

The parameter use in the smearing function is $\epsilon = 3\Delta z$ where Δz is the reference grid size in the axis direction. Based on the hypothesis of blade elements, the body forces of rotor blade can be achieved through the airfoil data and the flow field information.

The actuator disc solves the entire axisymmetric flow field and as such the induced velocity is naturally included into the formulation, i.e., the relative velocity and flow angle are determined from

$$\phi = \tan^{-1} \left(\frac{V_0 - W_z}{\Omega r + W_\theta} \right), V_{rel}^2 = (V_0 - W_z)^2 + (\Omega r + W_\theta)^2 \quad (6)$$

The local angle of attack is given by $\alpha = \phi - \gamma$, where γ is the local pitch angle. The lift and drag forces per spanwise length are found from tabulated airfoil data.

$$L = \frac{1}{2} \rho V_{rel}^2 c BC_l, \quad D = \frac{1}{2} \rho V_{rel}^2 c BC_d \quad (7)$$

The forces are calculated in every iteration such that the momentum equation produces new velocity field at each time iteration which updates the flow angle of attack.

2.2 BPM noise generation method

The semi-empirical airfoil self-noise model of Brooks et al. [3] was developed by scaling the experimental data using the NACA 0012 airfoil. The method was extended for wind turbine aerodynamic noise generation [4] and is applied for the current study. In order to generalize the model, the boundary layer thickness is modelled with Xfoil rather than using the original data based on the NACA 0012 airfoil. A general form of BPM model reads

$$SPL = 10 \log_{10} \left(\frac{\delta M^{n_{LD}}}{r^2} \right) + G_1(St) + G_2(Re) + G_3(\delta) + C. \quad (8)$$

It is seen in equation (8) that airfoil noise is a function of thickness parameter δ , either relating to the boundary layer thickness or blunt TE thickness. The length parameter l represents the span length of an airfoil. Other functions, such as G_1 , G_2 and G_3 are related to the Strouhal number, Reynolds number and boundary layer thickness parameters. More detailed formulation of individual noise mechanisms is referred to [3,4]. The BPM model can be activated either at the meanwhile when the RANS/AD is running or after the flowfield is stabilized. For both cases, the relative velocity and angle of attack at each blade element are fed into the BPM model. When the local Reynolds number and angles of attack at each blade element are obtained, the boundary layer thickness at trailing edge is interpolated from the existing database. Such a database was prepared using Xfoil computations for a wide range of angles of attack and Reynolds numbers. The prepared boundary layer thickness database also considers clean and rough airfoil surface conditions, such that wind turbine noise under free transition and leading edge separation can be modelled.

2.3 PE noise propagation method

With the effect of ambient flow, the speed of sound is written as $c_{eff} = c + v_x$ where v_x is the wind velocity component between source and receiver. The velocity component may come from field measurement, analytical expression or numerical simulation. With an assumption of constant density distribution, the PE equation reads

$$\left[\nabla^2 + k^2(1 + \epsilon) - \frac{2i}{\omega} \frac{\partial v_i}{\partial x_j} \frac{\partial^2}{\partial x_i \partial x_j} + \frac{2ik}{c_0} \mathbf{v} \cdot \nabla \right] P'(r) = 0 \quad (9)$$

where $\epsilon = \omega/c_0$, ω is the radian frequency of the sound, c_0 is the reference speed of sound, $P'(r)$ is the monochromatic sound pressure field, and $\epsilon = (c_0/c)^2 - 1$. The equation is reduced to the classical Helmholtz equation without the effect from ambient flow. The wind turbine noise source is located at a certain height in the domain as shown in Figure 1. The source is smeared along the vertical direction which is called starting field. The PE equation is solved along the x-direction. The amplitude of the sound pressure is updated from $P(x)$ to $P(x+\Delta x)$. More details of mathematical manipulation of the PE equation is referred to [5].

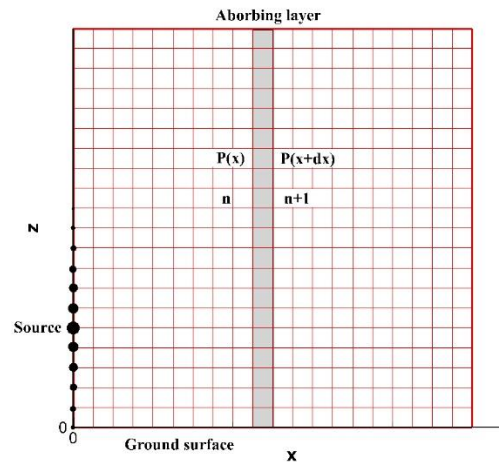


Figure 1. Typical grid in the propagation plane used in the PE method.

From the results of subsection 2.1 and 2.2, the total wind turbine noise spectrum is summed up from each blade element such that

$$L_p(f) = 10 \log_{10} \left(\sum_i^n 10^{0.1 SPL_{total}^i} \right) \quad (10)$$

where the total aerodynamic noise is added for n blade elements and SPL_{total}^i is the total noise from airfoil elements i . The wind turbine sound pressure level $L_p(f)$ is the initial condition for calculating long range noise propagation. An integrated value of $L_p(f)$ over surface is called sound power level $L_w(f)$ that is a more general description of noise strength. Ideally, $L_w(f)$ does not change with distance, such that the propagation loss can be expressed as

$$L_p(f) = L_w(f) - 10 \log_{10} 4\pi D^2 - \alpha D + \Delta L \quad (11)$$

The quantity ΔL is called relative sound pressure level which is the main focus of the present study. Any deviation from the noise source can be represented by ΔL such as ground reflection, atmospheric refraction, atmospheric turbulence, irregular terrain, noise barriers and so on. The term $10 \log_{10} 4\pi D^2$ is called geometric attenuation which is corresponding to spherical spreading of sound waves from a point source. The effect from atmospheric absorption is calculated with the term αD , which is the combined effect from absorption coefficient and propagation distance. To clearly distinguish wind turbine noise propagation due to turbulent flow effect, only the relative sound pressure level ΔL is presented in the current study.

The total sound pressure level is fitted to the PE domain as an initial condition, such that both the wind turbine noise source and wake flow are integrated in the noise propagation solver. The numerical solution of the PE is based on frequency domain. At each frequency, there is a corresponding sound pressure level obtained from the total wind turbine noise spectrum. The noise source is located at hub height. To avoid numerical singularity, the noise source is smeared along the vertical direction at the boundary ($x=0$ m). More details about noise source starting field are referred to Salomons [5]. The horizontal boundary of the computational domain is fixed at $x=1000$ m. In the vertical direction, the choose of domain height actually varies with the frequency to be solved. The basic requirement of mesh resolution is $\Delta x = \Delta z = \lambda/8$ which means that each sound wave should cover at least 8 mesh points. In this sense, the domain height is usually larger for lower frequencies. It is worth mentioning that the CFD domain is slightly larger than the PE domain such that the required flow variables are not missing in the PE computations.

3. Results and discussions

This section first provides a benchmark sound propagation study. Multiple wind turbine flow, noise generation and propagation under various flow conditions are studied in details. For each frequency, the relative sound pressure level ΔL is calculated over long distance. Finally, the original sound pressure level of the source is compared with the noise spectra at receiver.

3.1 Validation of long-range sound propagation over a hill

This test case considers irregular terrain and moving medium effect. The terrain contains flat surface and a Gaussian hill of 10m maximum height. The ground and hill are both the absorbing ground surfaces that have same flow resistivity of $200 \text{ kPa} \cdot \text{s} \cdot \text{m}^{-2}$. For typical grassland, the flow resistivity varies between $100 \text{ kPa} \cdot \text{s} \cdot \text{m}^{-2}$ and $300 \text{ kPa} \cdot \text{s} \cdot \text{m}^{-2}$. Sound speed in the moving medium is given by a logarithmic function

$$c_{eff}(z) = c_0 + b \ln\left(\frac{z}{z_0} + 1\right) \quad (12)$$

where c_{eff} is the effective sound profile along the vertical direction, the standard sound speed $c_0=340$ m/s and the roughness height is assumed $z_0 = 0.1 \text{ m}$. Here in this case, $b = 1$ represents slight downward atmospheric refraction. In Figure 2, the relative sound pressure level ΔL is computed at a frequency of 300Hz. In the PE computational domain, the presence of the hill had significant effect for sound propagation, especially near the ground. The ΔL values at a receiver height of 2 m is compared with the results using the Greens function parabolic equation method [5].

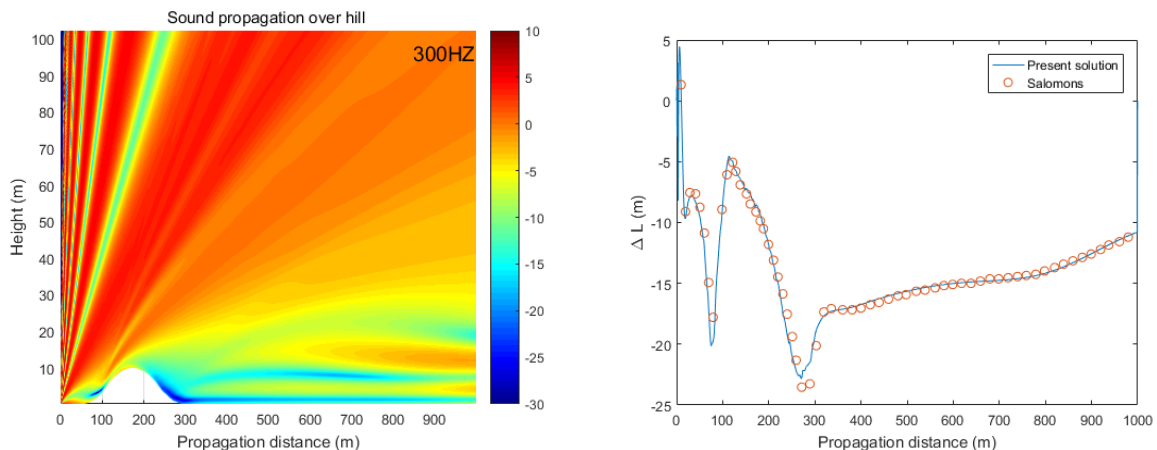


Figure 2. Sound propagation over a hill: Comparison between results from Salomons [5].

3.2 Flow and noise coupled simulations

The wind turbine flow and acoustic simulations are carried out for the Vestas NM80 wind turbines. The key results from the AD simulation are the thrust and power coefficients, in addition to that, the angle of attack and relative velocity at each blade element form inputs to the BPM model. Similar as the BEM theory, the AD uses the tabulated airfoil data, but in spite of its approximate nature, the AD method not only exhibit good numerical accuracy and is much faster than the conventional mesh-based body-fitted rotor computations [10]. The flowfield is solved by the EllipSys2D code [12,13] which is a general purpose flow solver for incompressible flows.

The computational mesh and the typical wake flow behind a wind turbine cluster is shown in Figure 3. Since there is no wall boundary presented, the inflow boundary condition, the axisymmetric boundary condition and outflow boundary conditions are specified as 1,2,3, respectively, as shown in Figure 3(a). The number of mesh points in each block is 64×64 as indicated with red lines. The number of blocks used in the simulation depends on the number of wind turbines to be studied. In Figure 3(a), only two wind turbines are shown with the white lines. Ideally, the flow from the 2D axisymmetric computation has exactly the same solution as 3D computation. There have been

numerous studies on modelling wind turbine wake with different numerical approaches. It is not of our interest in the present study to go into more details.

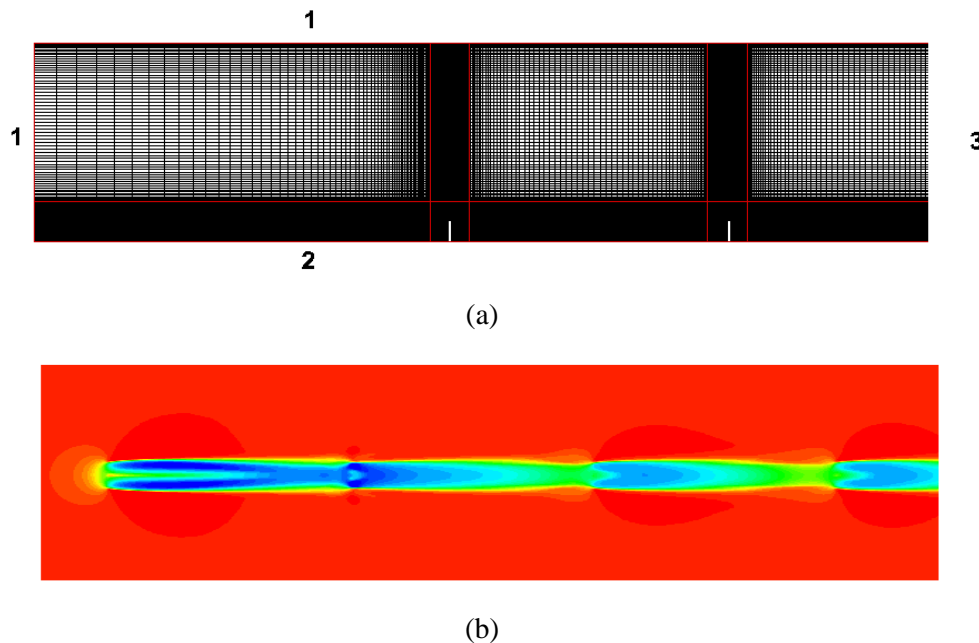


Figure 3. (a) The mesh topology; (b) The simulated flowfield behind the NM80 wind turbines.

Practically, each wind turbine has different inflow condition due to the wake effect, such that the noise sources of each wind turbine can be calculated. At a wind speed of 8 m/s, the sound pressure level of the Vestas NM80 wind turbine is calculated. The detailed noise spectra are shown in Figure 4, the total noise spectrum (SPL-TOTAL) is summarized from all other noise mechanisms such as inflow noise (SPL-INFLOW), turbulent boundary layer trailing edge noise (SPL-TBLTE), flow separation noise (SPL-SEPARATION), laminar boundary layer vortex shedding noise (SPL-LBLVS), trailing edge bluntness noise (SPL-TEBLUNT) and blade tip noise (SPL-TIP). It is seen that the inflow noise contains large amount of low frequency noise components where the TE noise sources are dominate sources at middle to higher frequencies.

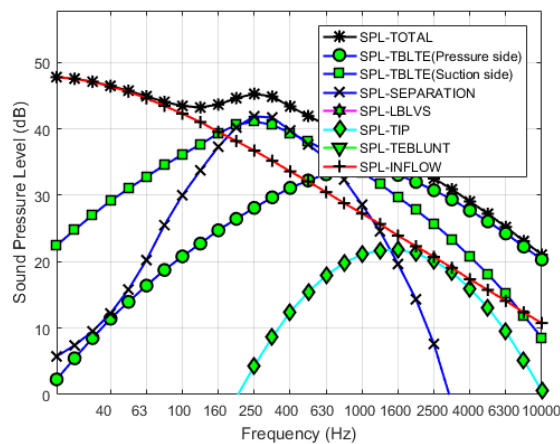
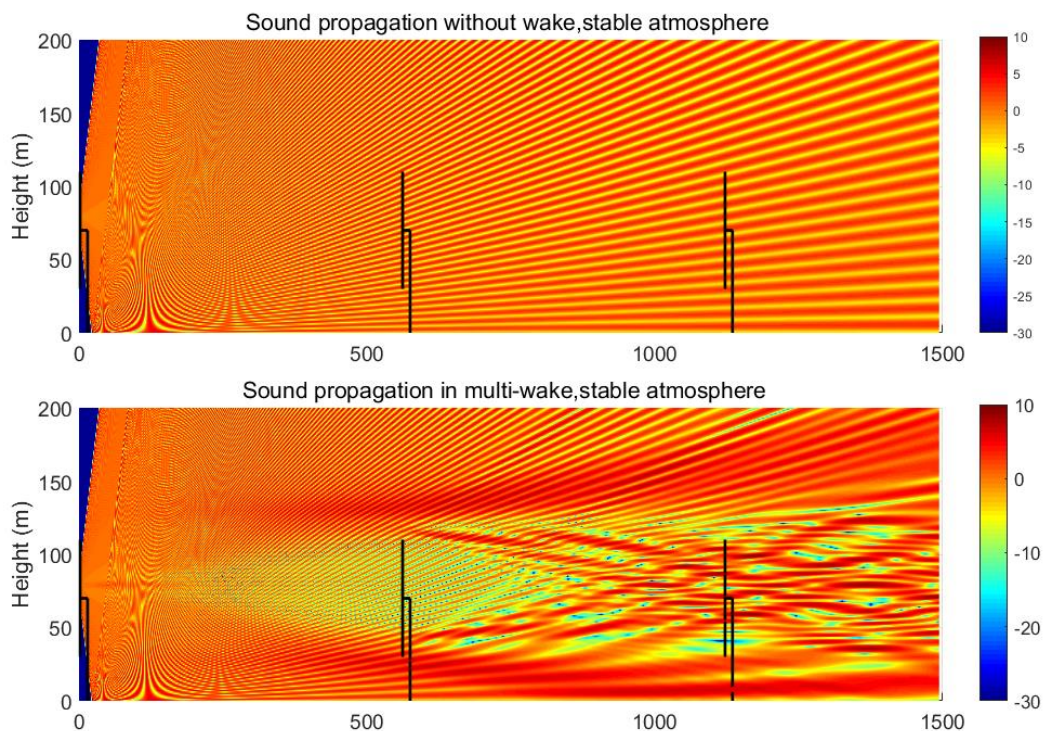


Figure 4. Aerodynamic noise sources of a single wind turbine.

Knowing the flow solutions and neglecting other propagation losses, the aforementioned relative sound pressure level ΔL is then ready to be simulated. In Figure 5, the relative sound pressure level ΔL

over a distance of 1500 m is simulated at a frequency of 300 Hz. The three wind turbines are located at $x=0, 560$ and 1120 m which have relatively large spacing between each other. The wind turbine noise source is located at $(x, z)=(0 \text{ m}, 70 \text{ m})$. To clearly see the propagation effects through multi-wake, the noise sources from the other two wind turbines are not involved. From the top, the simulated cases are: (1) Sound propagation in stable atmosphere ($b=0$) and without the wake effect; (2) Sound propagation in a stable atmosphere ($b=0$) and with the multi-wake influence; (3) Sound propagation in a downward refracting atmosphere ($b=3$) and with the multi-wake influence; (4) Sound propagation in an upward refracting atmosphere ($b=-3$) and with the multi-wake influence. It is clearly seen in Figure 5 that sound propagation is strongly influenced by the presence of complex flowfield. In the first case, the ground absorption and reflection play role. In the second case, wind turbine noise from the first wind turbine propagates through all three wind turbine wakes under stable atmosphere. The contour plot of ΔL largely deviates from the first solution. In the third case, when the downward refraction is presented, there is a strong ‘noise pollution’ at long range behind the third wind turbine. In addition, a small quiet zone is seen at the distance of $x=1000$ m. A much quieter situation is shown in the fourth simulation where the upward refraction is assumed. In this case, a large quiet zone is seen after the second wind turbine and is extended until $x=1500$ m. It is worth mentioning that in the (aerodynamic) calculations uniform inflow is considered but (in case of $b \neq 0$) an altitude dependent variation of (temperature) and speed of sound (but not of the inflow wind speed) is taken into account in the propagation calculation. Also, the wind turbines sketched in the figure is only an illustration, the flow is absolutely axisymmetric without any shear or tower shadow effect.



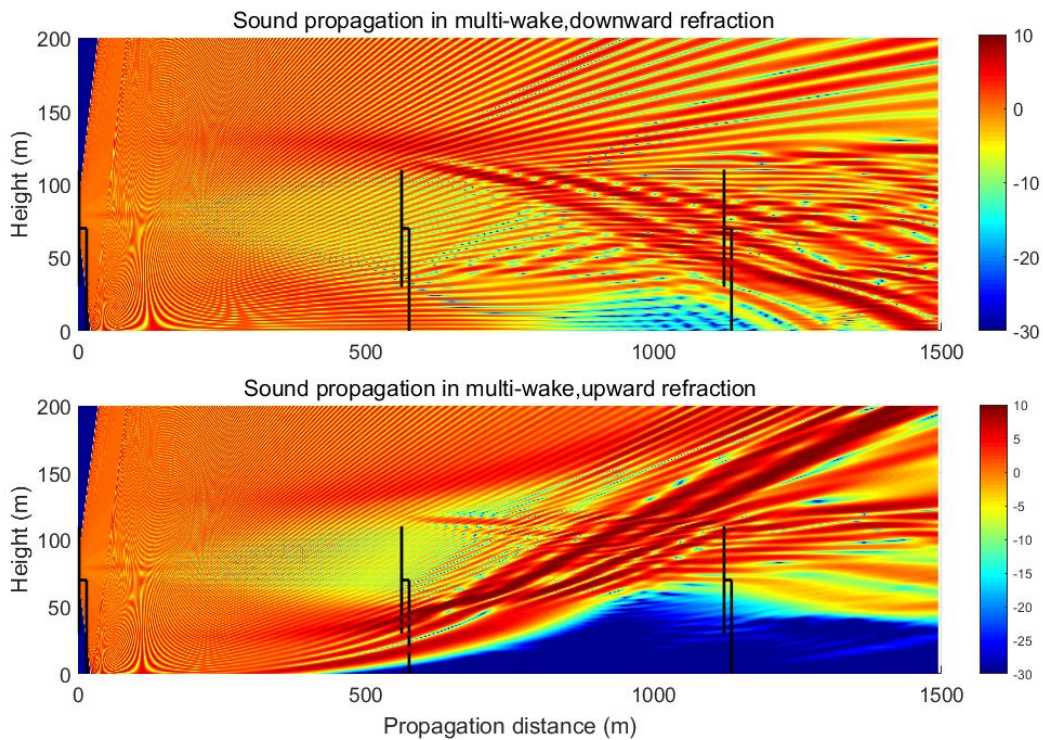


Figure 5. Wind turbine sound propagation: (a) stable atmosphere without wake effect; (b) stable atmosphere through multi-wake; (c) downward refracting atmosphere and multi-wake; (d) upward refracting atmosphere and multi-wake.

To evaluate the detailed changes of ΔL , a closer look of relative sound pressure level at a receiver height of $h=2$ m is presented in Figure 6. In case 1, since there is no refraction presented, at longer propagation distance, the reflection effect becomes very weak, the ΔL tends to become a constant value. In other cases, ΔL varies significantly over propagation path at $h=2$ m. A large propagation loss is seen at $x=1500$ m for case 4 where as in case 3, ΔL slightly increase due to strong downward refraction. It is worth noting that, the ΔL values at different height can be significantly different which can be extracted from pressure contours shown in Figure 5. From these comparisons, it is obvious that wind turbine noise propagation largely depends on the ambient conditions. As shown in Figure 6, in the near field ($x < 500$ m) the variation of sound pressure is much smaller as compared with sound pressure at far field ($x > 500$ m). This highlights the importance of far field sound prediction under complex atmospheric conditions.

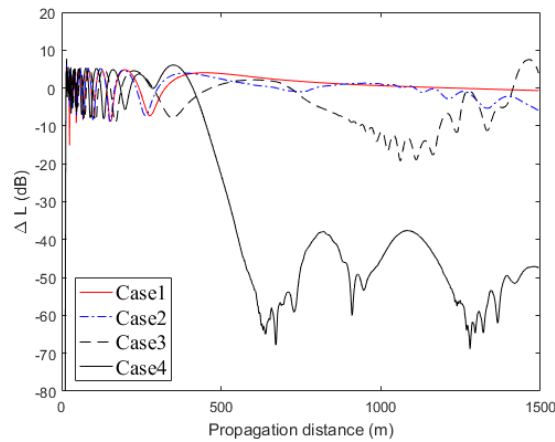


Figure 6. The relative sound pressure levels for a receiver at 2m height under four different atmospheric conditions discussed above.

The same numerical procedure can be repeated for noise propagation at other frequencies. In the current work, the wind turbine noise source propagation in 1/3-octave band is simulated from 20Hz to 5000Hz. It is known that the computational effort becomes larger at higher frequencies. For example, the mesh points used for $f=3000$ Hz is typically 100 times more than that is used for $f=300$ Hz. Therefore frequencies above 5000 Hz are not considered here. Another reason is that sound waves at high frequency can be significantly absorbed by air where the corresponding atmospheric absorption coefficient α is large. The original noise spectrum is obtained at the 2D downstream location. If the propagation loss from ΔL is not considered, one can easily compute the sound pressure spectrum at $x=1500$ m using Equation 11 with $\Delta L = 0$. Otherwise, if ΔL is computed at all desired frequencies, the full effect from long range propagation can be obtained. The wind turbine sound pressure level near source location and at $x=1500$ m are gathered in Figure 7. It is seen that the most significant propagation loss is due to the geometrical attenuation. The air absorption is seen to have larger influence at $f > 1000$ Hz. Case 1 results some increase of SPL at low frequencies whereas Case 3 shows continues noise increase at $f > 200$ Hz.

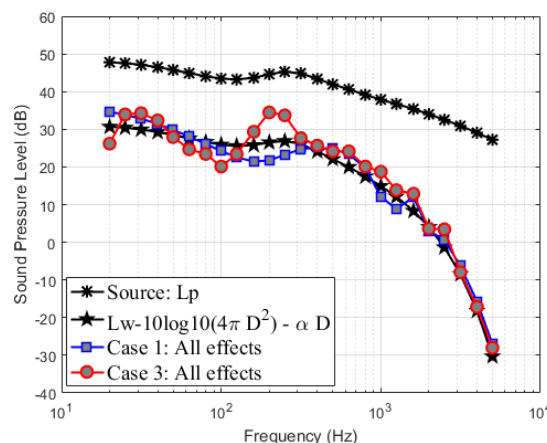


Figure 7. Sound pressure level at 2 rotor diameter downstream of the first wind turbine (Source: Lp) and at 1500 m distance: with geometric attenuation and air absorption, Case 1 and Case 3 with all propagation effects.

4. Conclusion

In this study, an integrated numerical method for multi-wind turbines flow and aerodynamic noise prediction is presented. The numerical simulations are based on the existing flow solver EllipSys2D where the wind turbine noise source model and noise propagation model are integrated with flow solver. With the advantage of the 2D axisymmetric AD solver, the steady flowfield is obtained very efficiently. The wind turbine noise source is computed based on the flow information. The noise source propagation is then investigated considering the flowfield as an input for the PE simulations. Results under different flow conditions revealed that long-range wind turbine noise propagation behaves significantly different with atmospheric stability and wake flow.

Acknowledgements

The authors wish to express acknowledgement to the National Nature Science Foundation under grant number 11672261, the Key Laboratory of Wind Energy Utilization, Chinese Academy of Sciences under grant number KLWEU-2017-0201 and the Jiangsu Province Natural Science Foundation (BK20160476).

References

- [1] Glauret H. 1935 *Airplane propellers*. Springer, , 169-360.
- [2] Sørensen JN, Shen WZ. 2002 *Numerical modeling of wind turbine wakes*. Journal of Fluids Engineering. 124.
- [3] Brooks TF, Pope, DS, Marcolini MA. 1989 *Airfoil Self-Noise and Prediction*. NASA Reference Publication 1218, National Aeronautics and Space Administration, USA.
- [4] Zhu WJ, Heilskov N, Shen WZ, Sørensen JN. 2005 *Modeling of aerodynamically generated noise from wind turbines*. Journal of Solar Energy Engineering. 127: 517-528.
- [5] Salomons EM. 2001 *Computational Atmospheric Acoustics*. Springer Science Business Media B. V.
- [6] Barlas E, Zhu WJ, Shen WZ, Dag KO, Moriarty P. 2017 *Consistent modelling of wind turbine noise propagation from source to receiver*. The Journal of the Acoustic Society of America, 142(5) 3297. DOI: 10.1121/1.5012747.
- [7] Lee S, Lee D, Honho S. 2015 *Prediction of far-field wind turbine noise propagation with parabolic equation*. In: 21st AIAA/CEAS Aeroacoustics Conference, Dallas, Texas.
- [8] Heimann D, Kaasler Y, Gross G. 2011 *The wake of a wind turbine and its influence on sound propagation*. Meteorologische Zeitschrift, 20: 449-460.
- [9] Barlas E, Zhu WJ, Shen WZ, Sørensen JN, Kelly M, Andersen SJ. 2017 *Effect of wind turbine wake on atmospheric sound propagation*. Applied Acoustics, 122:51-61.
- [10] Mikkelsen R. 2003 *Actuator Disc Methods Applied To Wind Turbines*. MEK-FM-PHD 2003-02. Technical University of Denmark.
- [11] Michelsen JA. 1992 *Basis3D – A Platform for Development of Multiblock PDE Solvers*. Technical Report AFM 1992-05; Technical University of Denmark.
- [12] Sørensen NN. 1995 *General Purpose Flow Solver Applied Over Hills*. RISØ-R-827-(EN) 1995; Risø National Laboratory, Denmark.